3D Magnetic Field Responses to a Defect Using a Tangential Driver-coil for Pulsed Eddy Current Testing

Yu-hua ZHANG [1], Hui-xian SUN [1], Fei-lu LUO [1]

[1] National University of Defense Technology; Changsha, China
Phone: +86 0731 4574994; e-mail: zhangyuhua@nudt.edu.cn, flluo@nudt.edu.cn

Abstract: In Pulsed Eddy Current (PEC) testing, the response feature of one-dimensional magnetic field component, perpendicular to the conductor's surface, is used to detect and quantify the defects. It is not sufficient for signal interpretation and noise suppression. A novel PEC probe, which consists of a tangential driver-coil and three orthorhombic pickup coils, is introduced in this paper. It is greatly advantageous to realize three dimensional field components measurement independently. Moreover it is characteristic of self-difference and lower lift-off noise. Using Finite Element Method (FEM), three dimensional magnetic flux density responses due to a defect in conductor plate, have been calculated. The result shows that a defect's depth and edges can be evaluated quantitatively by extracting three dimensional field components responses features. Numerical predication is in good agreement with experimental measurement. These merits are valuable for imaging inspection of defects (such as corrosion, dent, rivet hole, etc) in the aircraft structures.

Keywords: Pulsed eddy current testing, Tangential driver-coil, Three-dimensional magnetic field measurement, Response feature, Quantitative evaluation, self-difference

1. Introduction

Pulsed eddy current testing is arousing interest for the detection of cracks and corrosion in ageing metallic aircraft structure[1-5]. Typically, a pulse eddy current probe is composed of a cylindrical driver coil and a smaller pick-up coil or a magnetic field sensor [1-3, 6-7]. The driver coil, carrying on a pulse current, induces a broadband electromagnetic pulse to propagate through a conducting material. The pick-up coil or magnetic sensor senses the changing field, perpendicular to the conducting material, as a transient response in the time domain. Generally, the signal peak, the time to peak or zero-crossing are extracted for defect detection and identification [1, 6-8]. In order to obtain more information to improve detectability of pulsed eddy current testing for surface/subsurface defects, a novel probe, which consists of a tangential driver-coil and three orthorhombic pickup coils, is introduced in this paper. The merits of the proposed probe are that it is greatly advantageous to pickup three-dimensional magnetic field components for detection, and is characteristic of self-difference. In the following section 2, the electromagnetic field distribution characteristics and eddy current flow pattern, produced by a tangential driver coil have been investigated by 3-D finite element method. In section 3, 3-D magnetic field responses to a defect in conductor plate, have been analyzed. By peak features of three dimensional field components responses, a defect's depth and edges can be evaluated quantitatively. Experiments and results are presented in Section 4. Finally, conclusions and further work are outlined.

2. Probe modeling and its characteristics

2.1 Problem formulation

A tangential coil above a conducting plate is shown in Figure 1. Considering the orientation of the coil to the conducting plate, a Cartesian coordinate system is introduced here and its origin is located in the center of the plate surface. The coil axis is parallel to the plane *z=0*, which is coincided with the plate surface. The coil is wound with N wire turns and is driven by a pulse current, with time constant $\tau = 30\mu s$, duty ratio $t_0 = 0.5$ and period $T = 10ms$. The dimension of the plate, $a = b = 5L$, is adequately larger than the tangential coil that plate edge effect on the eddy current flow can be neglected. The problem domain is restricted to a finite range in $-10L \le x, y, z \le 10L$. A homogeneous Dirichlet condition for the magnetic field is imposed on the outer boundaries ($x, y, z = \pm 10L$). The basic equation for 3-D eddy current problem based on the $A-\phi$ method, is given by[9]

$$\nabla \times \frac{1}{\mu} \nabla \times \vec{A} - \nabla (\frac{1}{\mu} \nabla \cdot \vec{A}) + \sigma \frac{\partial \vec{A}}{\partial t} + \sigma \nabla \phi = 0 \quad \text{in the conductor} \qquad (1)$$

$$\nabla \left(\sigma \frac{\partial \vec{A}}{\partial t} + \sigma \nabla \phi \right) = 0 \quad \text{in the conductor} \qquad (2)$$

$$\nabla \times \frac{1}{\mu_0} \nabla \times \vec{A} - \nabla (\frac{1}{\mu_0} \nabla \cdot \vec{A}) = \vec{J}_s \quad \text{in the air} \qquad (3)$$

Where $\vec{A}$ is the magnetic vector potential, ϕ electric scalar potential, $\vec{J}_s$ is the source current density, μ_0 is the free-space permeability, σ and μ are material conductivity and permeability separately.

Taken into consideration of source current characteristic, this is 3-D transient eddy current problem and can be solved based on variable time-step method. Using Finite element software ANSYS, the electromagnetic field and eddy current have been calculated at time interval Δt during $T/2$, Δt is chosen as *0.01ms* in the transition period and *0.1mm* in the steady state according to current change rate.

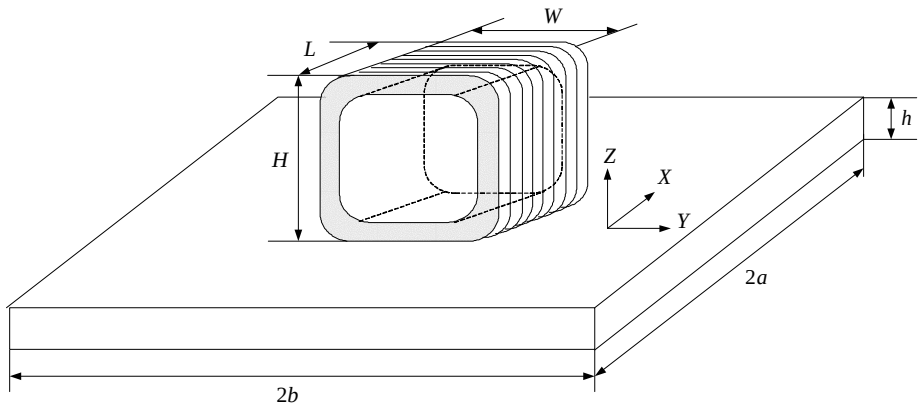

Figure 1 Schematic diagram of a tangential driver-coil to a conducting plate

2.2 Flow pattern of eddy current produced by a tangential driver-coil

When unimpeded by the intrusion of material boundaries or discontinuities, eddy-current

distribution characteristic is determined by the orientation of the probe-coil to the test material. Figure 2 (a) shows that the distribution of the eddy current induced by a cylindrical driver-coil. Eddy currents flow paths are circular and parallel to the turns of the coil and perpendicular to the axis of the coil's flux field. In the central region of the conducting plate, eddy current is self-canceling, that makes its density very small there, and decays rapidly to zero as the depth is increasing[10]. The maximal eddy current density appears in the adjoining region to the coil diameter. So, it is a rule that the flaw size, which is larger than or compared with the diameter of a cylindrical coil, can be detectable[11]. As shown in Figure 2(b), eddy currents, produced by a tangential driver-coil, flow uniform underneath the coil and tend to circular pattern on either side of the coil. In the central rectangle region of the conductor, the eddy-current density is approximately equal and maximum. Thus, it is greatly advantageous for small flaw detection, and makes the signal measured in self-difference. Moreover, this tangential coil is lower sensitive to lift-off [12].

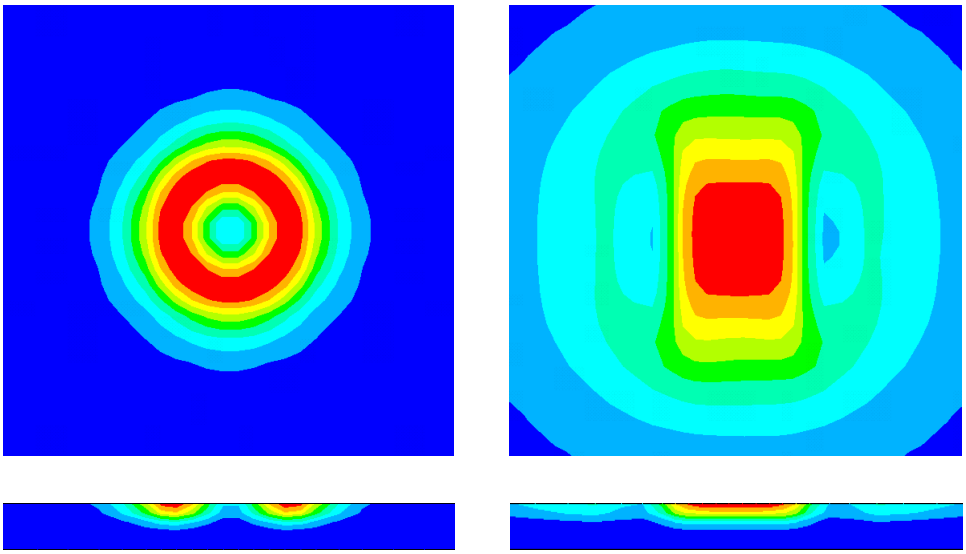

Figure 2 The distribution of eddy current induced by (a) a cylindrical coil (b) a tangential coil

2.3 The distribution characteristics of 3-D magnetic field components

The magnetic flux density at locations (*-5.0mm≤x≤5.0mm, y=0, z=0.25mm*) and (*x=0, -5.0mm≤y≤5.0mm, z=0.25mm*), are listed in Table I. It is obvious that the magnetic field, B_{sum}, changes slightly and is considered as to approximately equal in the extent (*-5.0mm≤x, y≤5.0mm*). Furthermore, the relationship of three magnetic field components, B_x, B_y and B_z is expressed as : $B_x >> B_y$, $B_x >> B_z$ and $B_x \approx B_{sum}$. B_y and B_z is almost equal to zero and B_x is uniform. These characteristics are determined by the coil configuration and orientation to the conductor and the extent of uniform field is varied closely by the coil dimensions. Table I is the results of magnetic field produced by a cylindrical coil with *L=40mm, W=25mm, H=25mm*.

Table I Magnetic flux density produced by a tangential driver-coil, t=0.26ms

(x,y,z) (mm)	$B_x(T)$	$B_y(T)$	$B_z(T)$	$B_{sum}(T)$
(-5.0, 0, 0.25)	1.7959×10^{-2}	5.2807×10^{-6}	2.8804×10^{-4}	1.8181×10^{-2}
(-4.0, 0, 0.25)	1.8047×10^{-2}	3.3319×10^{-6}	2.1631×10^{-4}	1.8261×10^{-2}

(-3.0, 0, 0.25)	1.8136×10^{-2}	1.4146×10^{-6}	1.4506×10^{-4}	1.8341×10^{-2}
(-2.0, 0, 0.25)	1.8172×10^{-2}	1.425×10^{-6}	9.6920×10^{-5}	1.8374×10^{-2}
(-1.0, 0, 0.25)	1.8209×10^{-2}	4.0851×10^{-6}	4.8942×10^{-5}	1.8406×10^{-2}
(0, 0, 0.25)	1.8209×10^{-2}	4.2462×10^{-6}	1.3897×10^{-6}	1.8406×10^{-2}
(1.0, 0, 0.25)	1.8209×10^{-2}	4.4076×10^{-6}	5.1716×10^{-5}	1.8407×10^{-2}
(2.0, 0, 0.25)	1.8172×10^{-2}	2.3160×10^{-6}	9.9871×10^{-5}	1.8374×10^{-2}
(3.0, 0, 0.25)	1.8135×10^{-2}	5.3128×10^{-6}	1.4825×10^{-4}	1.8341×10^{-2}
(4.0, 0, 0.25)	1.8043×10^{-2}	1.5541×10^{-6}	2.2121×10^{-4}	1.8258×10^{-2}
(5.0, 0, 0.25)	1.7951×10^{-2}	2.6790×10^{-6}	2.9487×10^{-4}	1.8175×10^{-2}
(0, -5.0, 0.25)	1.7796×10^{-2}	4.1020×10^{-6}	1.6643×10^{-6}	1.8003×10^{-2}
(0, -4.0, 0.25)	1.7929×10^{-2}	3.1175×10^{-6}	1.8067×10^{-6}	1.8133×10^{-2}
(0, -3.0, 0.25)	1.8063×10^{-2}	2.1425×10^{-6}	3.5896×10^{-6}	1.8264×10^{-2}
(0, -2.0, 0.25)	1.8136×10^{-2}	8.0587×10^{-7}	2.8182×10^{-6}	1.8335×10^{-2}
(0, -1.0, 0.25)	1.8209×10^{-2}	3.0766×10^{-6}	2.1034×10^{-6}	1.8407×10^{-2}
(0, 0, 0.25)	1.8209×10^{-2}	4.2462×10^{-6}	1.3897×10^{-6}	1.8406×10^{-2}
(0, 1.0, 0.25)	1.8208×10^{-2}	5.4159×10^{-6}	7.3918×10^{-7}	1.8406×10^{-2}
(0, 2.0, 0.25)	1.8134×10^{-2}	4.7069×10^{-6}	1.2636×10^{-6}	1.8333×10^{-2}
(0, 3.0, 0.25)	1.8059×10^{-2}	4.1391×10^{-6}	2.5744×10^{-6}	1.8260×10^{-2}
(0, 4.0, 0.25)	1.7924×10^{-2}	4.9706×10^{-6}	2.2446×10^{-7}	1.8128×10^{-2}
(0, 5.0, 0.25)	1.7789×10^{-2}	5.8051×10^{-6}	2.8219×10^{-6}	1.7996×10^{-2}

3. The characteristics of the perturbed field by a defect

The magnetic field changes produced by a defect are shown in Figure 3. The dimension of defect, located in the center of aluminum plate, is *15mm×10mm×2mm*. The excitation current, in a tangential driver-coil with *40mm×25mm×25mm*, is clockwise. Thus, the uniform eddy-current flows toward +Y direction. In order to interpret the perturbed magnetic field accurately, the difference signal, $\triangle B_x$, $\triangle B_y$ and $\triangle B_z$, which are obtained by subtracting a reference signal from the defect signal are given in the air at *z=0.5mm*. It is observed that time responses of three difference signal at various locations change distinctly and decrease rapidly to zero in a short time after that the current is turned on. They are a series of pulse signal. We also observed that the uniform distribution of the field is disturbed intensely by a defect. $\triangle B_x$ sinks suddenly above the whole defect, $\triangle B_y$ and $\triangle B_z$ change like sine wave.

Generally, current flows into higher conductivity medium. So, the presence of a defect will divert eddy-current away from its original path. The uniform eddy-current, flowing toward +Y direction, deflects and concentrates along the defect's edge. The resultant magnetic field presents new characteristic as shown in Figure 3. $\triangle B_x$ appears a trough in that a portion of eddy-current flows the defect bottom. The deeper a defect is, the less the proportion of eddy-current, flowing along the defect bottom, is. Thus the deeper $\triangle B_x$ sinks. At the same time, a portion of eddy-current deflects clockwise or anticlockwise on the two sides of defect, and concentrates tightly near the defect ends. Consequently, $\triangle B_y$ and $\triangle B_z$ have a crest and a trough separately.

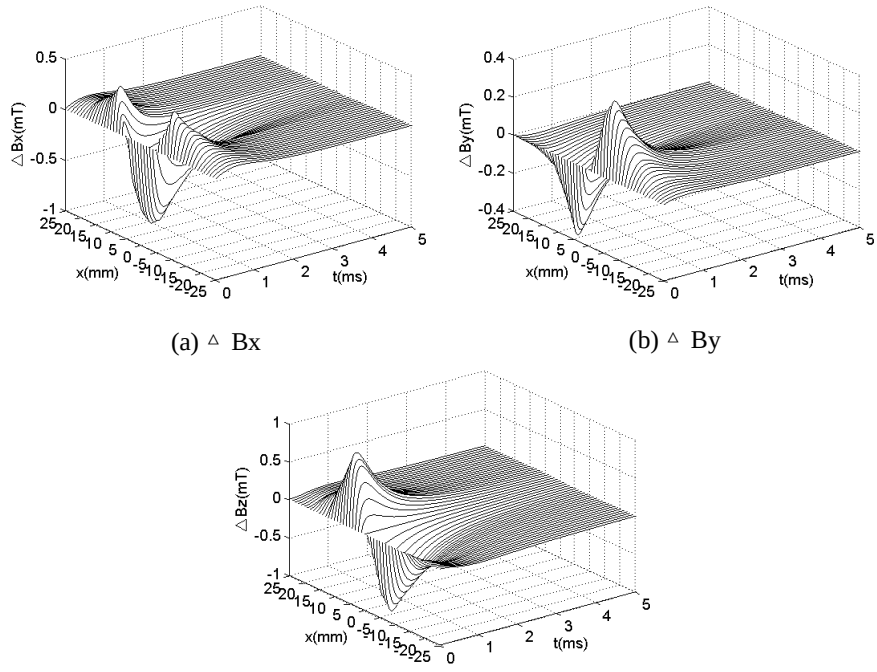

(a) △ Bx (b) △ By

(c) △ Bz

Figure 3 The characteristics of 3-D magnetic Field Components due to a defect (x=-25mm~25mm, y=0, z=0.5mm)

4. Experiments and discussions

In this experiment, a tangential driver-coil, with length *40mm*, width *25mm*, height *25mm* and *450* turns, is supplied by a amplitude *25 V*, frequency *100Hz* and duty ratio *0.5* pulse voltage. Three pick-up coils, shown in Table II, are fabricated to sensing three dimensional field change rate as induced voltage $U_{x,}$ U_y and U_z. Experiments are carried out for three defects in a aluminum plate. The dimensions of defects are as follows: *15mm×10mm×0.5mm (defect1)*, *15mm×10mm×1mm (defect2)* and *15mm×10mm×2mm (defect3)*.

Difference signals of three-dimensional induced voltage, $\triangle U_x$, $\triangle U_y$ and $\triangle U_z$, caused by defects are shown in Figure 4, 5 and 6. Unexceptionally, three transient responses are pulse signal in time domain. As the defect depth is deeper, the peaks of transient responses are larger. And $\triangle U_z$ is highly sensitive to depth variation. At a given time-point t_0, the scanning signals, as a function of distance to the defect, are shown. Figure 4(b) shows that $\triangle U_x$ tends to a broad trough along the whole defect. As shown in Figure 5(b), $\triangle U_y$ appears a crest and a trough as the probe is scanning along the defect width direction. The distance between crest and trough is approximately equal to defect width. Similarly, $\triangle U_z$ has a crest and a trough at the ends of the defect in Figure 6(b), the distance, from crest to trough, indicates the length of a defect. So, defect detection, using three dimensional field components, are achieved by the proposed pulsed eddy current probe.

Table II Dimensions of three pickup coils

pick-up coil	inner diameter	outer diameter	height	turns
x-axis	1.5mm	1.8mm	2.5mm	300
y-axis	1.5mm	2.9mm	2.5mm	900
z-axis	1.5mm	2.9mm	2.5mm	900

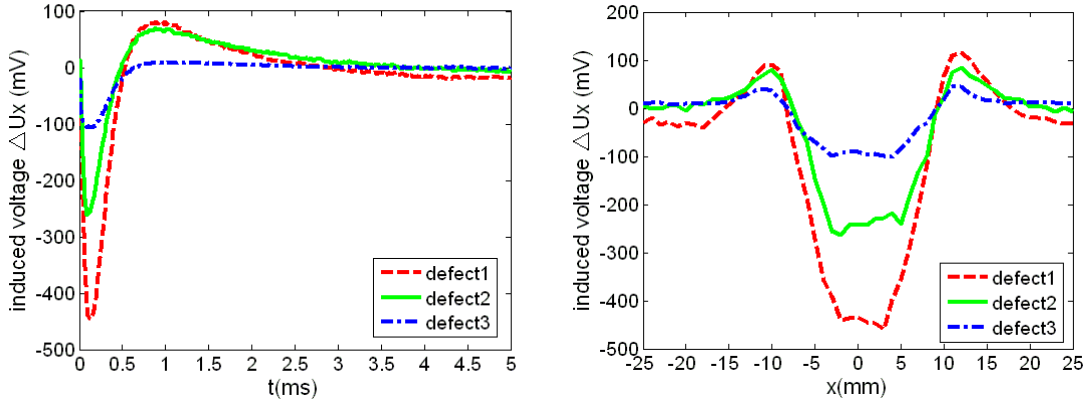

(a) (b)

Figure 4 (a) Transient response of $\triangle U_x$ at (x=0, y=0, z=1.25mm)

(b) $\triangle U_x$ as a function of distance to a defect (t=0.125ms, y=0)

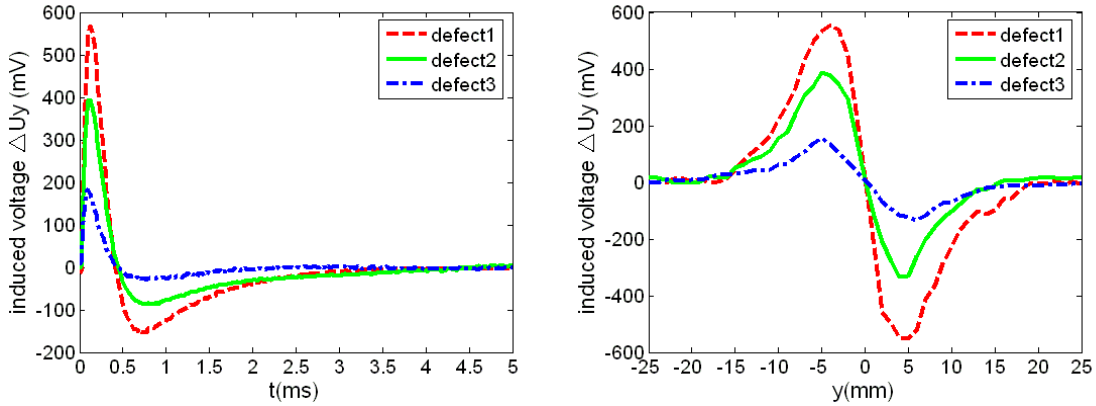

(a) (b)

Figure 5 (a) Transient response of $\triangle U_y$ at (x=-7.5mm, y=5mm, 1.25mm)

(b) $\triangle U_y$ as a function of distance to a defect (t=0.10ms, x=-7.5mm)

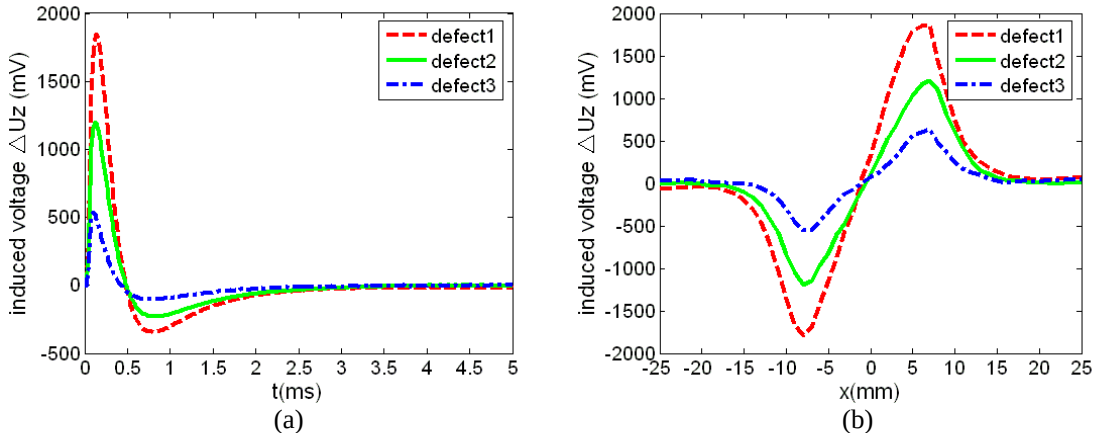

(a) (b)

Figure 6 (a) Transient response of $\triangle U_z$ at (x=-7.5mm, y=0, z=1.25mm)

(b) $\triangle U_z$ as a function of distance to a defect (t=0.10ms, y=0)

In the experiment, we also observed that induced voltage, U_x, is sufficiently stronger that U_y and U_z when there is on defect in the aluminum plate. But U_x is less sensitive to the presence of a defect than U_y and U_z. For example, $\triangle U_x / U_x$ is just 9.8%, $\triangle U_y / U_y$ is 100% and $\triangle U_z / U_z$ is 300%

for a defect with 2mm depth. Moreover, the amplitude of U_y and U_z is changing clearly as the probe is scanning along the defect. The probe is characteristic of self-difference in the y-direction, parallel to flow paths of the induced eddy current, and z-direction, perpendicular to the plate surface. So it is highly sensitive.

5. Conclusions

A novel pulsed eddy current testing probe, which consists of a tangential driver-coil and three orthorhombic pickup coils, is presented in this paper. The electromagnetic field distribution characteristics and eddy current flow pattern, produced by a tangential driver coil have been investigated by 3-D finite element method. The numerical results show that:

- The tangential probe is greatly advantageous to extract 3-dimensional magnetic field components changes for defect detection.
- It is characteristic of self-difference in the y-direction, parallel to flow paths of the induced eddy current, and z-direction, perpendicular to the test material surface. So it is highly sensitive.

Furthermore, 3-D magnetic field responses to a defect to a defect have been calculated and compared with the experimental results. The results show that a defect's depth and edges can be evaluated quantitatively by the features of the three-dimensional transient responses. These merits are valuable for imaging inspection of defects (such as corrosion, dent, rivet hole, etc) in the aircraft structures.

Reference

[1]. R. A. Smith, G. R. Hugo. Deep Corrosion and Crack Detection in Aircraft using Transient Eddy-current NDE[J]. Review of Progress in Quantitative NDE, 1999, pp1401~1408

[2]. B. A. Lepine, J. R. Giguère, D. S. Forsyth, etc. Applying Pulsed Eddy Current NDI to the Aircraft Hidden Corrosion Problem[C]. Proceedings of the Fifth Joint NASA/FAA/DoD Aging Aircraft Conference, 2001.

[3]. W. D. Rummel, J. R. Bowler. Integrated quantitative nondestructive evaluation (NDE) and reliability assessment of aging aircraft structures[R]. Final Report for the United States Air Force Office of Scientific Research., 2001.

[4]. B. F. Yang, F. L. Luo, Y. H. Zhang. Quantification and classification of cracks in aircraft multi-layered structure[J]. Chinese journal of mechanical engineering, 2006, Vol. 42, No.2, pp64-67.

[5]. J.Giguere, B.Lepine. Detection of Cracks Beneath Rivet Heads via Pulsed Eddy Current Technique[J]. Review of Quantitative Nondestructive Evaluation, 2002, Vol.21, pp1968-1975

[6]. Smith R A, Hugo G R. Transient eddy current NDE for ageing aircraft capabilities and limitations[J]. Insight, 2001, Vol.43, No.1, pp14-24.

[7]. G. I. Panaitov, H. J. Krause, Y. Zhang. Pulsed eddy current transient technique with HTS SQUID magnetometer for non-destructive evaluation[J]. Physica C 372-376, 2002,pp278-281

[8]. A. Sophian, G. Y. Tian, D.Taylor, ect. A Feature extraction technique based on principal component analysis for pulsed eddy current NDT[J]. NDT&E International, 2003, Vol36, pp37-41

[9]. Ansys Inc. Theory Reference manual. 2005.

[10]. H. Hoshikawa, K. Koyama. Eddy Current Distribution Using Parameters Normalized by Standard Penetration Depth[J]. Materials Evaluation, 1999, 7, pp587-593
[11]. C. J. Hellier Handbook of Nondestructive Evaluation [M].McGraw-Hill, 2003
[12]. T .P. Theodoulidis, E. E. Kriezis. Impedance Evaluation of Rectangular Coils for Eddy Current Testing of Planar Media[J]. NDT&E International 2005, 35, pp407-414.